Measurements of ${}^{4}_{\Lambda}\mathrm{H}$ and ${}^{4}_{\Lambda}\mathrm{He}$ Production in $\sqrt{s_{\mathrm{NN}}}$ = 3.0 - 3.5 GeV Au+Au Collisions at RHIC

Chenlu Hu[1,*] for STAR collaboration

[1]University of Chinese Academy of Science

Abstract. Hypernuclei, which are bound states of nuclei with at least one hyperon, serve as excellent experimental probes for studying the hyperon-nucleon (Y-N) interaction. In these proceedings, the measurements of A=4 hypernuclei (${}^{4}_{\Lambda}\mathrm{H}$ and ${}^{4}_{\Lambda}\mathrm{He}$) production from the RHIC-STAR experiment utilizing the fixed target datasets will be presented. The measured yields dN/dy of ${}^{4}_{\Lambda}\mathrm{H}$ and ${}^{4}_{\Lambda}\mathrm{He}$ as a function of rapidity will be shown from $\sqrt{s_{\mathrm{NN}}}$ = 3.0, 3.2 and 3.5 GeV Au+Au collisions. Additionally, the energy dependencies of the ratio of ${}^{4}_{\Lambda}\mathrm{H}/\Lambda$ and ${}^{4}_{\Lambda}\mathrm{He}/\Lambda$ will be examined to explore isospin effects. The mass dependence of the mean transverse momentum $<p_{\mathrm{T}}>$ will be also discussed. Furthermore, calculations from PHQMD, thermal model and transport model JAM plus coalescence afterburner will be compared to these results and the relevant physics implications will be discussed.

1 Introduction

Relativistic heavy ion collisions are an abundant source of strangeness. As strange quarks have to be newly produced during the hot and dense stage of the collision, they are thought of carrying information on the properties of the matter that was created[1, 2]. Hypernuclei, which consist of at least one hyperon, serve as an excellent experimental tools for studying the hyperon-nucleon (Y-N) interaction. It is well known that Y-N interactions, especially at high baryon density, are not only essential for understanding the inner structure of compact stars[3, 4], but also for describing the hadronic phase of heavy-ion collisions. Heavy-ion collisions provide an environment where it is possible to study the Y-N interaction under finite temperature and density conditions through measurements of hypernuclei properties, such as their collective flow and production yields.

A=4 mirror hypernuclei (${}^{4}_{\Lambda}\mathrm{H}$ and ${}^{4}_{\Lambda}\mathrm{He}$) are substantially tighter bound states compared to the hypertriton (${}^{3}_{\Lambda}\mathrm{H}$). The existence of the spin-1 excited states (${}^{4}_{\Lambda}\mathrm{H}^{*}(1^{+})$ and ${}^{4}_{\Lambda}\mathrm{He}^{*}(1^{+})$)[5] may also enhance the measured yields through feed-down. As such, their yields allow us to gain insight on the effects of hypernuclear binding, spin and isospin content on their production in heavy-ion collisions. In these proceedings, the yields dN/dy and mean transverse momentum p_{T} spectra of ${}^{4}_{\Lambda}\mathrm{H}$ and ${}^{4}_{\Lambda}\mathrm{He}$ in Au+Au collisions at $\sqrt{s_{\mathrm{NN}}}$ = 3.0 - 3.5 GeV will be discussed.

*e-mail: huchenlu@ucas.ac.cn

2 Experimental and Data Analysis

The STAR experiment carried out the Beam Energy Scan (BES) program in order to study the properties of quark-gluon plasma (QGP) and search for quantum chromodynamics (QCD) critical point. In BES-II program, by fixed-target (FXT) mode, the center of mass collision energy extends from 7.7 GeV down to 3.0 GeV.

In this analysis, we used the dataset of Au + Au collisions at $\sqrt{s_{\mathrm{NN}}}$ = 3.0 - 3.5 GeV collected using the FXT setup at RHIC by the STAR experiment. We mainly used Time Projection Chamber (TPC) detector for particle identification. The hypernuclei ${}^{4}_{\Lambda}$H and ${}^{4}_{\Lambda}$He are reconstructed with following decay channels: ${}^{4}_{\Lambda}\mathrm{H} \rightarrow {}^{4}\mathrm{He} + \pi^{-}$, ${}^{4}_{\Lambda}\mathrm{He} \rightarrow {}^{3}\mathrm{He} + \mathrm{p} + \pi^{-}$. The secondary decay topology is reconstructed by the KFParticle program which is based on a Kalman filter method[6]. In the program, the error-matrices are used to enhance the reconstruction significance. A set of cuts on topological variables are applied to the hypernuclei candidates to optimize the signal significance.

3 Results and Discussions

3.1 Particle Yields

The p_{T}-integrated yields dN/dy for ${}^{4}_{\Lambda}$H and ${}^{4}_{\Lambda}$He are calculated from the p_{T} spectra by combining data in the measured p_{T} range and function-fitting extrapolation in the unmeasured p_{T} range. Figure 1 presents the rapidity dependence of the dN/dy in 0-10% and 10-40% central Au + Au collisions across a range of $\sqrt{s_{\mathrm{NN}}}$ from 3.0 to 3.5 GeV. The rapidity distributions show slight variations, with a downward trend in central collisions and an increase towards backward rapidity in mid-central collisions. In 0-40% centrality, the ${}^{4}_{\Lambda}$He yield at mid-rapidity is comparable to that of ${}^{4}_{\Lambda}$H. The prediction from transport model Jet AA Microscopic (JAM) plus Coalescence[7, 8] is plotted for comparison. In the JAM+Coalescence model, the JAM transport model generates hadron phase space distributions at freezeout, followed by a coalescence procedure that forms (hyper)nuclei when the relative momentum and spatial distance of their constituents fall within defined limits. JAM+Coalescence calculations could describe the rapidity dependence of dN/dy for ${}^{4}_{\Lambda}$H in 0-40% centrality qualitatively.

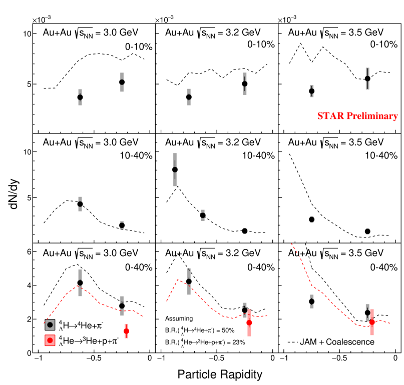

Figure 1. Rapidity distribution of ${}^{4}_{\Lambda}$H and ${}^{4}_{\Lambda}$He in 0-10% and 10-40% Au + Au collision at $\sqrt{s_{\mathrm{NN}}}$ = 3.0 - 3.5 GeV. The symbols represent measurements while the lines represent JAM+Coalescence calculations.

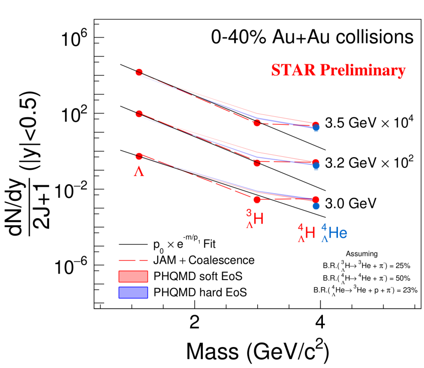

Figure 2. Mass dependence of measured dN/dy scaled by the spin degeneracy factor (2J+1). The symbols represent measurements while the lines represent different model calculations.

Figure 2 shows dN/dy for different particles scaled by their corresponding spin degeneracy factor 2J+1. The measured dN/dy exhibits an approximate exponential dependence on mass, but the yields of A=4 hypernuclei are above this trend shown as grey lines, which may explained by the feed-down from the excited states of ${}^{4}_{\Lambda}$H and ${}^{4}_{\Lambda}$He. Dashed lines are calculations from JAM+Coalescence afterburner, they shows a similar exponential dependence of $dN/dy/(2J+1)$ vs mass. Here, Λ is weighted to the data, and different coalescence parameters for ${}^{3}_{\Lambda}$H and ${}^{4}_{\Lambda}$H (${}^{4}_{\Lambda}$He) are needed to describe the data. The ΔR is 4.8 fm for both ${}^{3}_{\Lambda}$H and ${}^{4}_{\Lambda}$H (${}^{4}_{\Lambda}$He), and ΔP is 0.24 GeV/c for ${}^{3}_{\Lambda}$H and 0.38 GeV/c for ${}^{4}_{\Lambda}$H (${}^{4}_{\Lambda}$He). The larger ΔP may reflect of the tighter binding of A=4 hypernuclei. The Parton Hadron Quantum Molecular Dynamics (PHQMD)[9] approach could describe the yields of Λ, ${}^{4}_{\Lambda}$H and ${}^{4}_{\Lambda}$He, but overestimates that of ${}^{3}_{\Lambda}$H.

3.2 Particle Yield Ratios

Figure 3 presents the particle ratios of hypernuclei to hyperon (${}^{4}_{\Lambda}$H/Λ and ${}^{4}_{\Lambda}$He/Λ) as a function of collision energy. It shows the similar decreasing trend of ${}^{4}_{\Lambda}$H/Λ and ${}^{4}_{\Lambda}$He/Λ with the increasing energy. ${}^{4}_{\Lambda}$H/Λ is systematically larger than ${}^{4}_{\Lambda}$He/Λ probably because there are more neutrons than protons in the colliding system. The measured data are well described with JAM+Coalescence calculations, while overestimated by the Thermal-Fist[10].

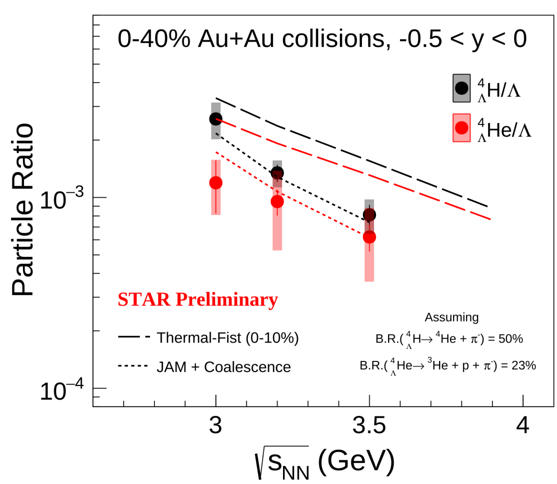

Figure 3. ${}^{4}_{\Lambda}$H/Λ and ${}^{4}_{\Lambda}$He/Λ at mid-rapdity in 0-40% central Au+Au collisions as function of the center of mass collision energy. The symbols represent measurements while the lines represent thermal model and JAM+Coalescence calculations.

3.3 Mean Transverse Momentum

Figure 4 presents the mass dependence of mid-rapidity $<p_T>$ for Λ, ${}^{3}_{\Lambda}$H, ${}^{4}_{\Lambda}$H and ${}^{4}_{\Lambda}$He, from the $\sqrt{s_{NN}}$ = 3.0 - 3.5 GeV in 0-10% and 0-40% Au+Au collisions. The measured $<p_T>$ follow the linear mass scaling up to 3.5 GeV, whcih is consistent with coalescence as the dominant process for hypernuclei production at mid-rapidity. Both JAM+Coalescence and PHQMD model could reproduce the mass dependence of $<p_T>$ qualitatively.

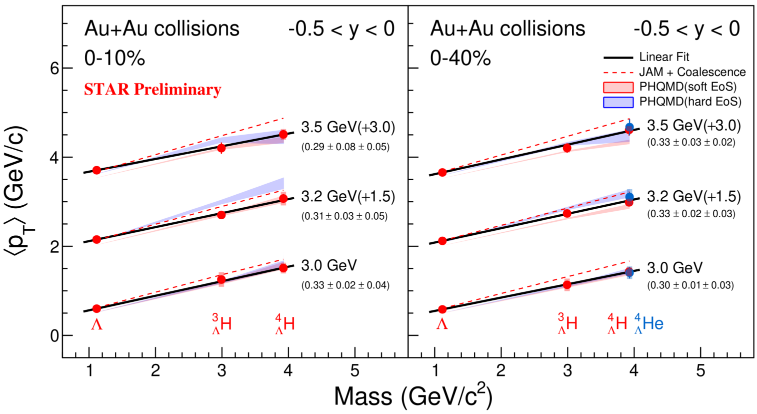

Figure 4. Mass dependence of the mid-rapidity $<p_T>$ for Λ, ${}^3_\Lambda$H, ${}^4_\Lambda$H and ${}^4_\Lambda$He, from the $\sqrt{s_{NN}}$ = 3.0 - 3.5 GeV in 0-10% and 0-40% Au+Au collisions. The symbols represent measurements while the lines represent JAM+Coalescence and PHQMD model calculations.

4 Summary and Outlook

In summary, we carry out the rapidity and centrality dependence measurement of ${}^4_\Lambda$H and ${}^4_\Lambda$He yields in Au+Au collisions from $\sqrt{s_{NN}}$ = 3.0 to 3.5 GeV in the high-baryon-density region. JAM+Coalescence model could qualitatively reproduce the rapidity and centrality dependence of ${}^4_\Lambda$H production. The yields of Λ, ${}^3_\Lambda$H, ${}^4_\Lambda$H and ${}^4_\Lambda$He do not strictly follow an exponential scaling with mass when divided by spin degeneracy, suggesting significant contributions from feed-down of excited A=4 hypernuclei. The ratio of ${}^4_\Lambda$H/Λ and ${}^4_\Lambda$He/Λ are well described with JAM+Coalescence calculations, while overestimated by Thermal-Fist. The linear mass scaling is observed in the mass dependence of mid-rapidity $<p_T>$ up to 3.5 GeV, which is well described by JAM+Coalescence afterburner and PHQMD calculations qualitatively. This is consistent with coalescence as the dominant process for hypernuclei production at mid-rapidity.

The results presented in these proceedings are based on a subset of the BES-II datasets. In Run 21, STAR collected 2 billion events at $\sqrt{s_{NN}}$ = 3 GeV. This larger dataset will enable measurements of heavier hypernuclei (A>4) and may help us gain valuable insights into the mass dependence of hypernuclei production.

References

[1] P. Koch, B. Muller and J. Rafelski, Phys. Rept. **142**, 167 (1986)
[2] J. Chen et al., (2024), arXiv:2407.02935 [nucl-ex]
[3] D. Gerstung, N. Kaiser, and W. Weise, Eur. Phys. J. **A56**, 175 (2020)
[4] D. Lonardoni et al., Phys. Rew. Lett. **114**, 092301 (2015)
[5] F. Schulz et al. (A1 Collaboration), Nucl. Phys. A **954** (2016), 149-160
[6] X. Y. Ju, Y. H. Leung, S. Radhakrishnann et al., Nucl. Sci. Tech. **34** (2023) 15
[7] Y. Nara, EPJ Web Conf. **208** (2019), 11004
[8] J. Steinheimer et al., Phys. Lett. B **714** (2012), 85-91
[9] S. Gläßel et al., Phys. Rev. C **105** (2022) no.1, 014908
[10] T. Reichert et al, Phys. Rev. C **107** (2023) no.1, 014912